1	Androctonus nazarii, a new species of scorpions from Khuzestan Province, Iran
2	(Scorpiones: Buthidae)

- 3 Fatemeh Salabi^{1,*}, Bahman Zangi², Alireza Forouzan¹, Mohammad Hossein Jahan-Mahin³,
- 4 Seyed Mahdi Kazemi³

- 1- Department of Venomous Animals and Anti-Venom Production, Razi Vaccine and Serum Research
 Institute, Agricultural Research, Education and Extension Organization (AREEO), Ahvaz, Iran.
- 8 **2-** Ghods Town, Tehran Province, Iran.
- 9 3- Zagros Herpetological Institute, 37156-88415, P. O. No 12, Somayyeh 14 Avenue, Qom, Iran
- *Corresponding author: Fatemeh Salabi, e-mail ID: f.salabi@rvsri.ac.ir

11

12

13

ABSTRACT

- 14 Recent research has clarified the historically complex taxonomy of the medically significant
- scorpion genus *Androctonus* in Iran, chiefly by resolving the *A. crassicauda* Olivier, 1807 species
- 16 complex and describing numerous new species. However, the taxonomic status of certain
- populations in Khuzestan Province (south-western Iran) has remained unsettled. Here, we describe
- a new species, *Androctonus nazarii* sp. nov., from Baghmalek in the Zagros Mountains of Khuzestan
- 19 Province, Iran. The new scorpion species, *Androctonus nazarii* sp. nov., is described from two male
- 20 specimens based on a suite of distinct morphological features. Its key diagnostic traits include a
- 21 brownish-yellow coloration, a light brown carapace without ocular black patches and with fine
- 22 granulation, uniformly yellow legs, and a specific yellowish-brown, finely granulated chela manus.
- The species is distinguished via detailed comparison with its closest relatives (A. crassicauda, A.
- 24 zagrosensis, A. sumericus, and A. barahoeii). Its discovery fills an important taxonomic gap in
- south-western Iran and carries significant implications for public health and conservation.
- 26 **Keywords:** Androctonus nazarii, Khuzestan Province, Morphological features, New species,
- 27 Zagros Mountains

1. Introduction

28

Iran harbors a remarkably diverse scorpion fauna, dominated by the family Buthidae [1, 2, 3, 4]. 29 This richness is fostered by the country's complex topography and diverse climates, which have 30 given rise to 18 recognized terrestrial ecoregions [5, 6, 7, 8]. The documented fauna includes 99 31 32 species from 20 genera, with a high rate of endemism (74 species). Within this fauna, the genus Androctonus Ehrenberg, 1828 is of critical medical importance due to the potent venom of its 33 species, representing a significant public health concern [9, 10]. The taxonomy of Androctonus has 34 long been challenging due to pronounced morphological convergence and high intraspecific 35 variation [11, 12]. This challenge was exemplified in Iran, where for decades diverse populations 36 were broadly classified under a single species, A. crassicauda [13, 1, 14]. Recent integrative 37 taxonomic studies have revolutionized this understanding, revealing that these populations represent 38 a complex of distinct species. This paradigm shift has prompted the description of numerous new 39 Androctonus species throughout the Middle East. Notable examples from the region now include A. 40 turkiyensis and A. kunti in Turkey, respectively [15]; A. ammoneus in Jordan [16]; A. omanensis and 41 A. ammophilus in Oman [17]; A. sumericus (Dhi Qar Province) and A. ishtar (Duhok and Nineveh 42 Provinces) in Iraq [18, 16]; A. tihamicus in Saudi Arabia [19]; and several from Iran, such as A. 43 sistanus, A. orientalis, and A. zagrosensis [20, 15, 10] from Iran. A comprehensive review by 44 Yağmur et al. [15] further resolved the taxonomy of *Prionurus crassicauda orientalis* Birula, 1900, 45 elevating it to species rank as A. rostami. Consequently, the genus now includes 49 species, with 46 nine currently recognized from Iran include: A. crassicauda (Olivier, 1807); A. orientalis (Birula, 47 1900); A. sistanus Barahoei and Mirshamsi, 2022; A. sumericus Al-Khazali and Yağmur, 2023; A. 48 transcaucasisus Kovařík, Yağmur, Fet and Lowe, 2025; A. azerianus Yağmur and Kovařík 2025; 49 50 A. caspius Kovařík, Yağmur, Fet and Lowe, 2025; A. barahoeii Kovařík and Yağmur, 2025, and A. 51 zagrosensis Kazemi and Salabi, 2025 [13, 15, 18, 20, 21, 22]. According to Kazemi et al., the genus Androctonus is one of two deadly genus scorpions of Iran [23]. Despite these significant advances, 52 53 the taxonomic status of *Androctonus* populations in several Iranian provinces, including Khuzestan, has remained unclear. Khuzestan Province, located in southwestern Iran, is a critical area of study. 54 55 It encompasses four distinct ecoregions—the South Iran Nubo-Sindian desert and semi-desert, the Tigris-Euphrates alluvial salt marsh, the Zagros Mountains forest steppe, and the Arabian Desert 56 and East Saharo-Arabian xeric shrublands—whose ecological convergence supports an 57 exceptionally rich scorpion fauna. The province is home to over 30 species, representing 58

approximately one-third of Iran's total diversity [8, 24]. Although recent work has begun to clarify its diversity, with species such as *A. zagrosensis*, *A. barahoeii*, and *A. sumericus* being described from the province, significant gaps in our understanding persist. Here, we describe a previously unreported species, *A. nazarii* sp. nov., from Baghmalek, Khuzestan, whose medical importance was previously unassessed. We investigate this population by comparing it morphologically with its closest relatives, including *A. crassicauda*, *A. zagrosensis*, *A. sumericus*, and *A. barahoeii*.

2. Material and Methods

65

66

2.1. Specimen collection

- Approximately 50 specimens of *Androctonus* sp. were collected at night using ultraviolet light detection in Baghmalek, Khuzestan Province, Iran, in August 2025 (Figures 1, 2). Based on distinct
- 69 morphological coloration, two individuals were selected and preserved in 96% ethanol for
- 70 morphological analyses. Voucher specimens, including the holotype (mature male) and paratype
- 71 (immature male) of A. nazarii sp. nov., have been deposited in the Venomous Animals Museum of
- 72 the Razi Vaccine and Serum Research Institute, Karaj, Alborz, Iran.

73 **2.2.** Morphological analysis

- 74 Morphological examination was conducted on two males (one mature, one immature) using a Leica
- 75 MZ 7.5 stereomicroscope. The assessment followed the taxonomic frameworks of Sissom et al. [25]
- and Yağmur [26], with a focus on coloration, pedipalp morphology, and prosomal/metasomal
- 77 features. Standardized imaging was performed according to the protocol of Yağmur [26].
- 78 Morphometric data, comprising six meristic traits and 18 morphometric ratios, were recorded in
- 79 millimeters (mm) using digital calipers.

80 2.3. Abbreviations of Morphometric Ratios.

- 81 CL: Carapace length; CPW: Carapace posterior wide; CAW: Carapace anterior wide; CHL: Manus+
- fixed finger length; ML: Manus length; MFL: Movable finger length; No.MFT: Number of Movable
- fig teeth (L: left; R: right); No.FFT: Number of fixed finger teeth (L: left; R: right); No.PT: Number
- of Pectinal teeth (L: left; R: right); Body Length: BL; Mt(I-V)L: metasomal segment I-V length;
- 85 Mt(I-V)W: metasomal segment I-V wide; RVSRI; Razi Vaccine and Serum Research Institute;

VAMRVSRI: Venomous Animals Museum of Razi Vaccine and Serum Research Institute, Karaj, Alborz, Iran.

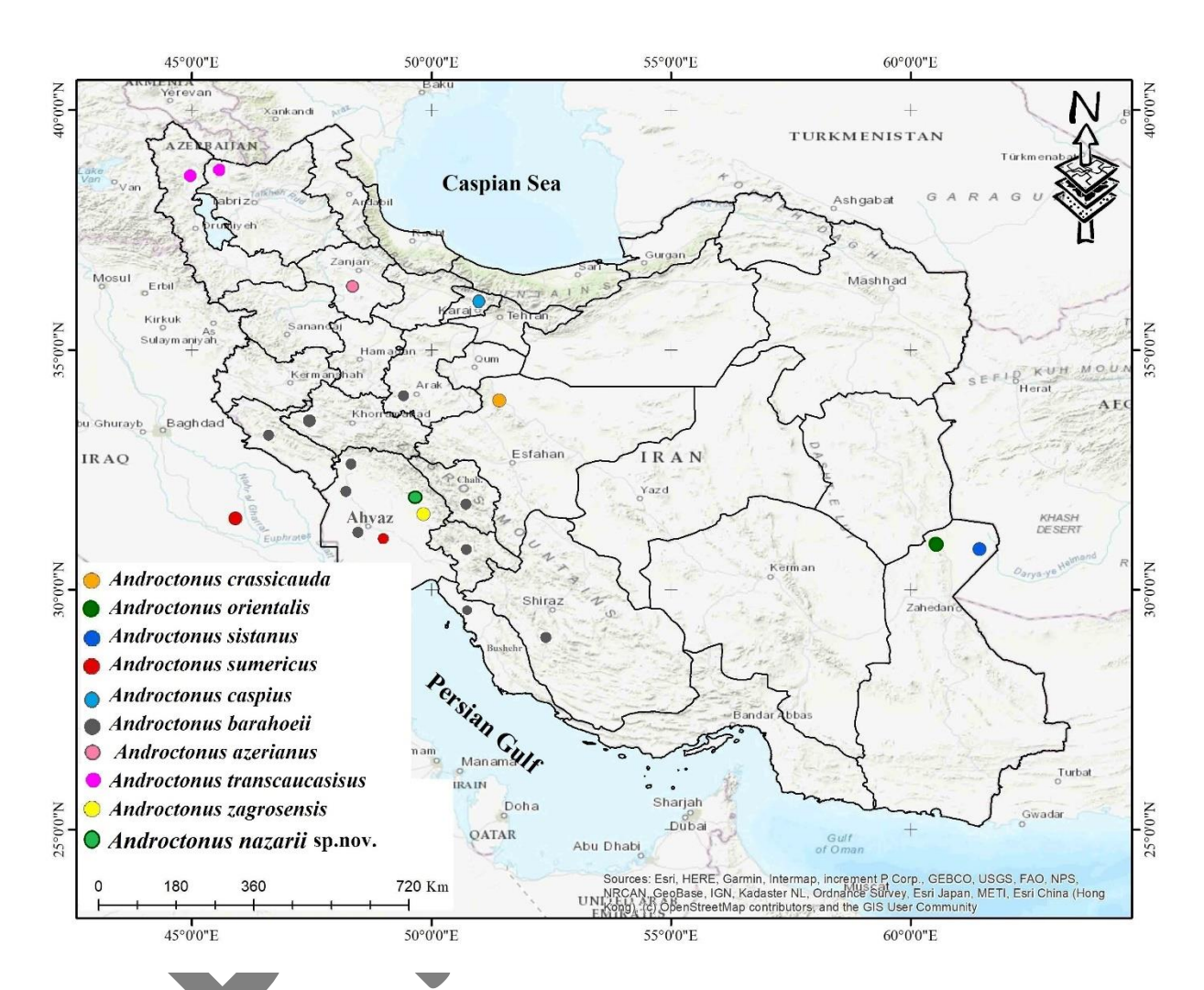


Figure 1. Localities of *Androctonus* genus in Iran and sampling area of *Androctonus nazarii* sp. nov. from Baghmalek, Khuzestan, Iran.

3. Results

3.1. Systematic description

Order Scorpiones C.L. Koch, 1837

Family Buthidae C.L. Koch, 1837

- 99 Genus Androctonus Ehrenberg, 1828
- 100 Androctonus nazarii sp. nov. (Figures 2–10)
- Material examined (2 specimens including 2 males)
- Holotype: 1♂ (VAMRVSRI, catalog number VAMRVSRI-SA010), Iran, Khuzestan Province,
- Baghmalek, Qaleh tol, 10 km NW of Qaleh tol, 31.618°N, 49.961°E, elev. 800 m, 15 September
- 2025, leg. F. Salabi. Paratypes: 16 (same locality as holotype, 15 September 2025, leg. F. Salabi
- 105 leg.
- 106 **Etymology**
- The species epithet is a patronym honoring Mahmood Nazari for his contributions to scorpion
- taxonomy and diversity in Khuzestan, Iran.
- 109 Type locality
- 110 Iran, Khuzestan Province, Baghmalek, Qaleh tol.
- 111 Geographical distribution
- Populations of this species are distributed in the southwestern Iran, Baghmalek, Bakhmali region
- 113 (Qaleh tol to AblashkareOlya).
- 114 **Diagnosis** (1♂ holotype)
- A. nazarii sp. nov. is a medium-sized species (adult body length 66.88 mm). The base color light
- brown to brownish-yellow; the ocular area surrounding the median eyes and the lateral eyes lacks a
- distinctive black patch; pedipalps, metasomal segments I–V and telson brownish-yellow; legs
- uniformly yellow, without any spots in males. A unique feature of this scorpion is the high-contrast
- black carinae found on parts of its carapace, pedipalps, and metasoma. The pectinal tooth count 27–
- 28. The carapace exhibits dense, fine granulation, lacking large granules. The pedipalps are stocky.
- 121 Femur. Pentacarinate; all carinae well-developed and granular; intercarinal surfaces with scattered
- granules; the external surface becoming mostly smooth posteriorly. *Patella*. Octocarinate; dorsal,
- ventral, and external surfaces smooth or with very few scattered granules; internal surface finely
- granulated; dorsal prolateral and ventral prolateral carinae strongly crenulated, bearing coarse,
- pointed, conical granules, each demarcated anteriorly by a large macroseta and associated with a

well-developed patellar spur; dorsal retrolateral and ventral retrolateral carinae weak to obsolete. The fixed and movable fingers possess 14–15 and 15–16 principal rows of denticles, respectively. *Sternite*. Sternites I-VII are uniformly light brown with dull yellow posterior margins; sternites I-VI are smooth and lack carinae, while sternite VII possesses four carinae on an otherwise smooth surface. *Metasoma*. Measoma I–V are smooth dorsally and laterally, granulate ventrally; segments I–V possess 10-8-8-8-5 carinae, respectively; the lateral inframedian carinae are complete on segment I, reduced to 4 coarse granules on II and 3 granules on III, and absent on IV–V. The fifth metasomal segment possesses moderately developed ventrolateral carinae, which bear granules that gradually and slightly increase in size posteriorly, culminating in four enlarged, rounded, and widely spaced granules. The dorsal carinae of segments I–IV and dorsolateral carinae of segments I–III are strong, bearing large, serrate granules that gradually increase in size posteriorly and end in two large posterior granules. The dorsolateral carinae of segment V have large, distinct, rounded anterior granules and no posterior granules. *Telson.* elongated; dorsally smooth with a pair of large symmetrical granules, ventrally granulate and ridged (Figure 2-10).

Table 1. Morphometric comparison of adult and immature males of *A. nazarii*.

Character	Species					
	∂-НТ	♂-PT				
CL	7.80	4.96				
CPW	7.63	4.71				
CAW	4.47	3.52				
CL/CPW	1.02	1.05				
CL/CAW	1.74	1.41				
CHL	13.01	9.99				
ML	5.35	3.64				
MFL	7.14	6.49				
Mt(I)L/W/D	5.16/5.35/4.81	3.27/3.55/3.03				
Mt(II)L/W/D	6.19/5.57/4.88	4.11/3.89/3.27				
Mt(III)L/W/D	6.76/5.83/5.1	4.17/3.94/3.42				
Mt(IV)L/W/D	7.66/5.68/5.25	5.14/3.90/3.56				
Mt(V)L/W/D	7.77/4.88/3.86	5.22/3.33/2.73				
Mt(I)L/W	0.96	0.92				
Mt(I)L/D	1.07	1.07				
Mt(II)L/W	1.11	1.06				
Mt(IV)L/D	1.46	1.44				

144	Mt(V)L/D	2.01	1.91
	TelsonL/W/H	7.02/2.87/2.23	4.59/1.91/1.7
	TL/W	2.45	2.40
	TL/D	3.15	2.7
	No.PT	27-28	26-27
	No.FFT	15	14
	No.MFT	16	15
	Met L	33.85	23.94
	Total body L	66.88	44.58
145			

149

150

151

152

153

154

155

156

157

158

159

160

161

162

163

164

165

166

167

147

Description (\mathcal{O}): Description is based on the 1 \mathcal{O} holotype (VAMRVSRI-AZ010) and the \mathcal{O}

paratype. 148

> **Coloration:** The body (from prosoma to telson) display differing pigmentation, ranging from brown to yellowish-brown and yellow (Figures 2, 3). Carapace. Predominantly brown, grading from a light anterior to a dark posterior; its carinae and granules are a darker shade, ranging from brown to blackish-brown. In males, the ocular area surrounding the median eyes lacks a distinctive black patch and the ocular area surrounding the lateral eyes lacks a color patch (Figures 3, 4); the median eyes themselves are uniformly light brown (Figures 3, 5). Chelicerae. Manus is yellowish-brown; fingers yellowish-brown with blackish-brown teeth. Pedipalps. The femur and patella are brownish-yellow on both the dorsal and ventral surfaces; their internal and external carinae are dark brown and feature brown median carinae and granules dorsally and ventrally (Figure 6); and the chela manus, and fingers are uniformly yellowish-brown (Figures 7, 8); denticles black. *Mesosoma*. Brown in male; the sternum, genital operculum, basal plate, and coxae are yellowish-brown; poststernites III–VII are brown with yellow margin (Figures 3, 5). The pectines are uniformly pale cream in color (Figure 3B). Metasoma. It appears yellowish-brown dorsally; yellowish-brown with light brown reticulations both laterally and ventrally; feature reddish brown carinae. Telson. The vesicle is yellowish-brown, while the aculeus is reddish-brown basally, reddish-black at tip (Figures 9). Legs. All segments are uniformly yellow, without any spots in adult male (Figure 10).

> Carapace and mesosoma: Carapace. The carapace of A. nazarii sp. nov. is trapezoidal, slightly longer than wide, with an almost straight anterior margin furnished with several stout macrosetae. In the adult male holotype, it measures 7.8 mm in length, with a length-to-posterior-width ratio of

1.02 and a length-to-anterior-width ratio of 1.74 (Table 1). The surface is dominated by multiple prominent carinae adorned with medium-sized, rounded granules. The intercarinal surfaces are densely covered with small granules, except for the predominantly smooth regions between the posterior median carinae and between and around the median eyes, which bear only finely scattered granules. The anterior region of the carapace features medium-sized, flattened granules. The median ocular tubercle is situated slightly anterior to the carapace center. The ratio of the distance from the median eye center to the anterior carapace margin versus the total carapace length is 0.40; the ratio to the posterior margin is 0.56. The median eyes are positioned on either side of the anterior median carinae and are separated by a distance of nearly two ocular diameters (Figures 3, 5). Five pairs of small, aligned lateral eyes are present, located above an area of finely granulated cuticle (Figure 5). Sternopectinal area. The sternum is pentagonal, longer than wide, and smooth. The genital operculum is longitudinally divided; in males, the two lateral plates are typically partially separated (Figures 3B). The pectines are long, densely setose, and extend beyond the coxatrochanter joint of leg IV. The pectinal tooth count in the adult male is 27–28, with each comb possessing 3 marginal and 7 median lamellae. Tergites. The tergites are densely granular. Tergites I-VI are tricarinate, with three moderate to strong carinae that project beyond the posterior margin. Their posterior margins also feature a distinct row of large, robust granules. The pretergites are finely granular, while the posttergites are more coarsely granular and moderately covered with rounded, moderate-sized granules, except between the lateral carinae where the fine granulation is denser. In contrast, tergite VII is smooth and pentacarinate. Its median carinae extend only halfway across the segment. All tergital carinae bear relatively large, rounded granules (Figures 3A, 4A). Sternites. Sternites III-VI are smooth, lack granules and carinae, and each bears a pair of vestigial furrows and ventral spiracles (Figures 3B, 4B). Notably, the superior portion of the sixth sternite's spiracle has distinct granulation. Sternite VII differs markedly, exhibiting two pairs of strong granular carinae while maintaining a smooth intercarinal surface.

168

169

170

171

172

173

174

175

176

177

178

179

180

181

182

183

184

185

186

187

188

189

190

191

192

193

194

195

196

197

198

Pedipalp: The pedipalps robust, of moderate length, and densely setose. *Femur*. The femur is moderately slender and pentacarinate, with all five carinae well-developed and bearing moderate granulation (Figure 6). The dorsal prolateral (dorsointernal), dorsal retrolateral (dorsoexternal), and ventral median carinae are strong and adorned with moderate, rounded granules; the ventral prolateral (ventrointernal) carina features distinct, coarse, spaced, and conical granules that are larger than those on adjacent carinae; the ventral retrolateral (ventroexternal) carina is strong and

bears moderate-sized, conical granules that become more spaced anteriorly. The dorsal intercarinal surface has scattered fine granules; the inner surface is covered with scattered granules of various sizes; the ventral surface bears very few granules of various sizes; the outer surface is covered anteriorly with a few irregular fine and coarse granules, has very few scattered fine granules on the posterior two-thirds, and lacks granules posteriorly (Figure 6). Patella. The patella is moderately slender, straight, and octocarinate. The dorsal, ventral, and external surfaces are smooth and lack granules, while the internal surface is covered with scattered fine granules. The dorsal prolateral (dorsointernal) carina is strong and strongly crenulated, bearing coarse, pointed, spaced, conical granules that decrease in size posteriorly; it is demarcated anteriorly by a large macroseta and accompanied by a well-developed dorsal patellar spur. The dorsal prolateral median carina is very strong with more developed corneation and bears distinct, moderate, rounded granules from anterior to posterior. The dorsal retrolateral median carina is moderately strong with moderate, rounded granules but is obsolete on the anterior one-fifth. The dorsal retrolateral (dorsoexternal) carina is weak, with indistinct and flattened granules, obsolete anteriorly, and curves posteriorly towards the dorsal retrolateral median carina. On the ventral side, the ventral prolateral (ventrointernal) carina is strong and granular, bearing relatively coarse and pointed, conical granules; it is demarcated anteriorly by a large macroseta and associated with a developed ventral patellar spur. The ventral prolateral median carina is very strong with more developed corneation and has regular, distinct, small, rounded granules. The ventral retrolateral median carina is moderately strong with rounded granules but is obsolete on the anterior and posterior one-fifth. The ventral retrolateral (ventroexternal) carina is smooth, lacks granules, and is obsolete anteriorly. Chela. Stocky; the manus is smooth on the dorsal, external, and ventral surfaces, without carinae; the internal surface is finely granulose. In the adult male, the manus length is 5.35 mm, and the movable finger length to manus length ratio is 1.33. The fingers are partly curved and moderately elongated, with the movable finger being 7.14 mm long in the adult male. The dorsal surface of the movable finger possesses fine setae, while the fixed finger lacks setae, except posteriorly. Both the pedipalp fixed and movable fingers are flanked by external and internal accessory denticles. The fixed and movable fingers possess 15–16 rows of denticles, complete with external and internal accessory granules; the movable finger also has three distal granules (Figure 6).

199

200

201

202

203

204

205

206

207

208

209

210

211

212

213

214

215

216

217

218

219

220

221

222

223

224

225

226

227

228

229

Metasoma and telson: The combined length of the metasoma and telson is 50.6–57.8% of the total body length in the adult male. *Metasoma*. Robust, dorsal surfaces of all segments smooth and

without setose, lateral and ventral surfaces very sparsely setose. Ventral surface of segment I smooth; segments II–IV smooth but with very few scattered fine to moderate granules, increasing slightly in density on segment IV; segment V smooth dorsally and laterally, but ventrally granulate with scattered moderate and fine granules. Segment I is longer than deep and occasionally wider than long. Segments II-V are longer than wide; segments I-V wider than deep. The width increases gradually from segment I to III, then decreases gradually from segment III to V. Segment V is the longest and least wide segment, whereas segment III is the widest. Morphometric ratios for the adult male are as follows: segment I length/width 0.96, length/depth 1.07; segment II length/width 1.11; segment IV length/depth 1.46; segment V length/width 1.59, length/depth 2.01. The dorsal furrow moderately deep and wide on all segments; metasoma exhibits a distinct pattern of serial carinal reduction: segment I has 10 carinae, comprising paired dorsal, dorsolateral, lateral inframedian, ventral median, and ventral lateral carinae; the lateral inframedian carinae are complete and moderate; segment II has 10 carinae, but the lateral inframedian are incomplete, present only on the posterior quarter as four granules. Segment III has 10 carinae, with the lateral inframedian reduced to three granules; segment IV has eight carinae (paired dorsal, dorsolateral, ventral median, and ventral lateral carinae); segment V has five carinae (paired dorsolateral and ventral lateral carinae, and a single ventral median carina). The dorsal carinae are paired on segments I-IV, strong, and bear serrate granules that are slightly enlarged posteriorly; on segments II-IV, the dorsal carinae terminate in two enlarged, acuminate granules, which achieve their maximum development on segment IV; the posterior end of the dorsal carina on segments II and III features one or two small granules spaced apart from the terminal, largest granule, while on segment IV it ends directly with the largest granule; this carina is absent on segment V. The dorsolateral carinae are paired on all segments; on segments I–IV they are strong with rounded granules, while on segment V they are strong, bearing very rounded granules anteriorly that fuse and become smooth posteriorly. The ventral median carinae are strong and of moderate development on segments I-V, bearing moderately rounded granules; they are paired on segments I-IV and single on segment V. Paired ventral lateral carinae are present on all metasomal segments, strong on segments I–IV and bearing large, rounded granules; on segment V, the carinae remain strong, with granules that gradually enlarge posteriorly and feature four terminal granules that are markedly enlarged and widely spaced (Figure 9). The lateral inframedian carinae are subject to serial reduction: fully developed and strong on segment I, they are represented by four coarse granules on segment II, only three granules on

230

231

232

233234

235

236

237

238

239

240

241

242

243

244

245

246

247

248

249

250

251

252

253

254

255

256

257

258

259

segment III, and are entirely absent from segments IV and V (Figure 9). *Telson*. The telson is slender and elongate, with a setose, ridged, and granulated ventral surface and a smooth dorsal surface (Figure 9); the aculeus is robust, elongate, and moderately curved. In the adult male, the telson is 7.02 mm long, with a length/width ratio of 2.45 and a length/depth ratio of 3.15 (Figure 9).

Legs: long, slender, covered with macrosetae; the tarsus, basitarsus, and tibiae of legs I–IV are densely covered dorsally and ventrally; the femur and patella of legs I and II are also covered dorsally and ventrally. In contrast, the femur and patella of legs III and IV are covered only ventrally. The patella of these segments has only a few bristle combs, while the femur has relatively very few bristle combs dorsally (Figure 10).



Figure 2. Holotype specimen of *Androctonus nazarii* sp. nov. from Baghmalek, Khuzestan, Iran. A. Dorsal view. B. Ventral view (Scale bar: 10 mm).

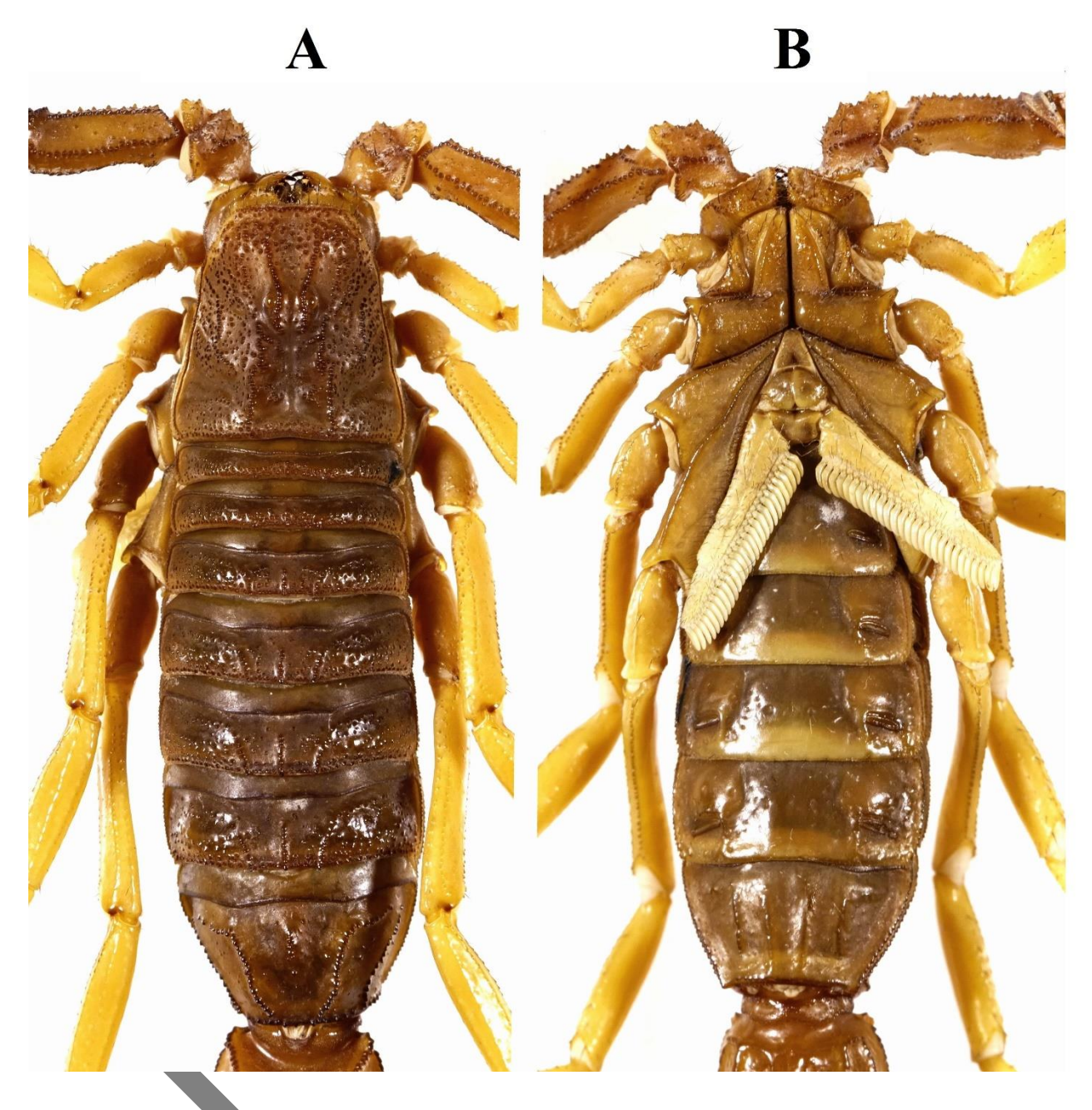


Figure 3. Holotype specimen of *Androctonus nazarii* sp. nov. from Baghmalek, Khuzestan, Iran. A. Carapace and mesosoma B. Sternopectinal area and ventral of mesosoma.

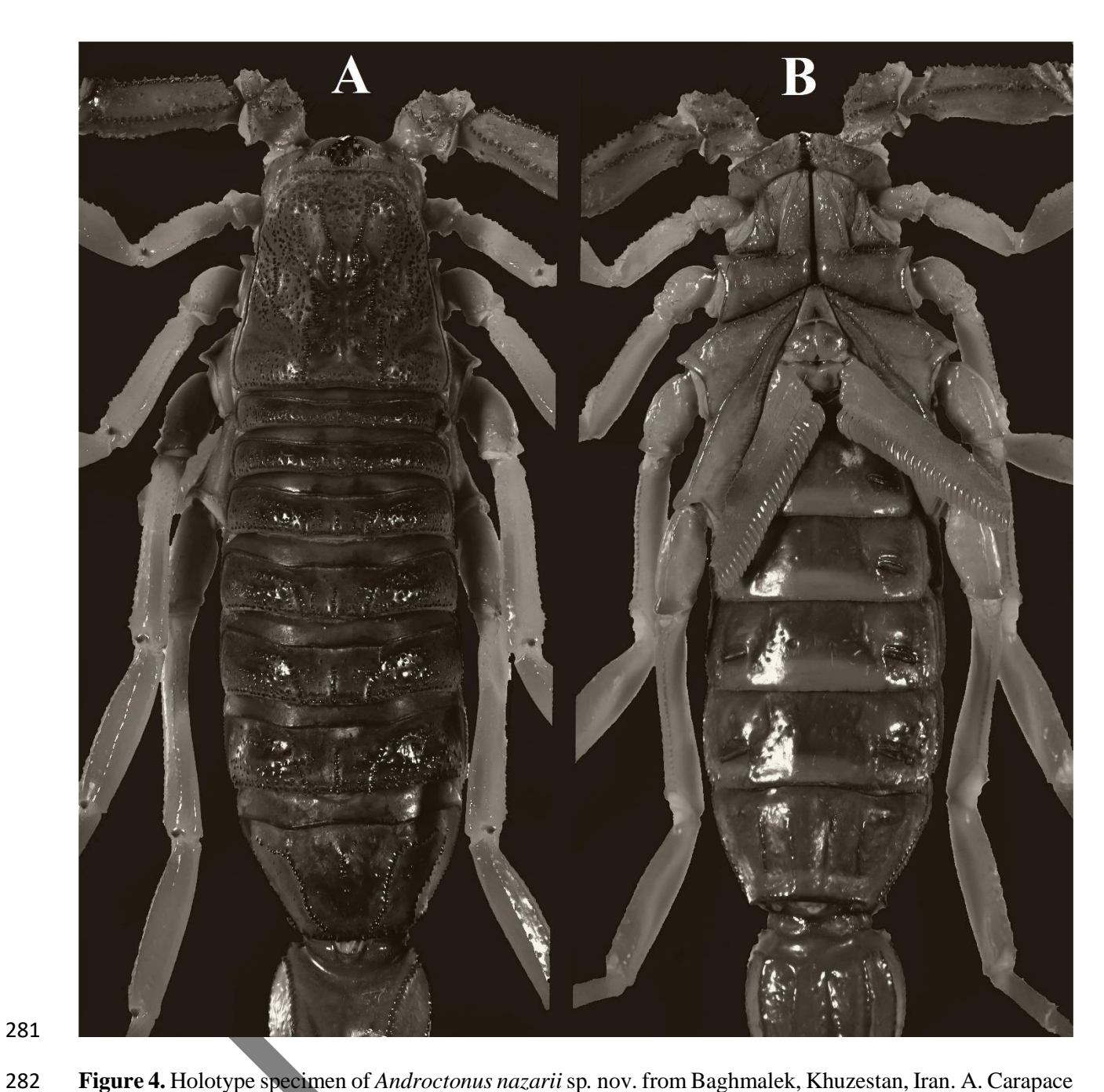


Figure 4. Holotype specimen of *Androctonus nazarii* sp. nov. from Baghmalek, Khuzestan, Iran. A. Carapace and mesosoma B. Sternopectinal area and ventral of mesosoma.

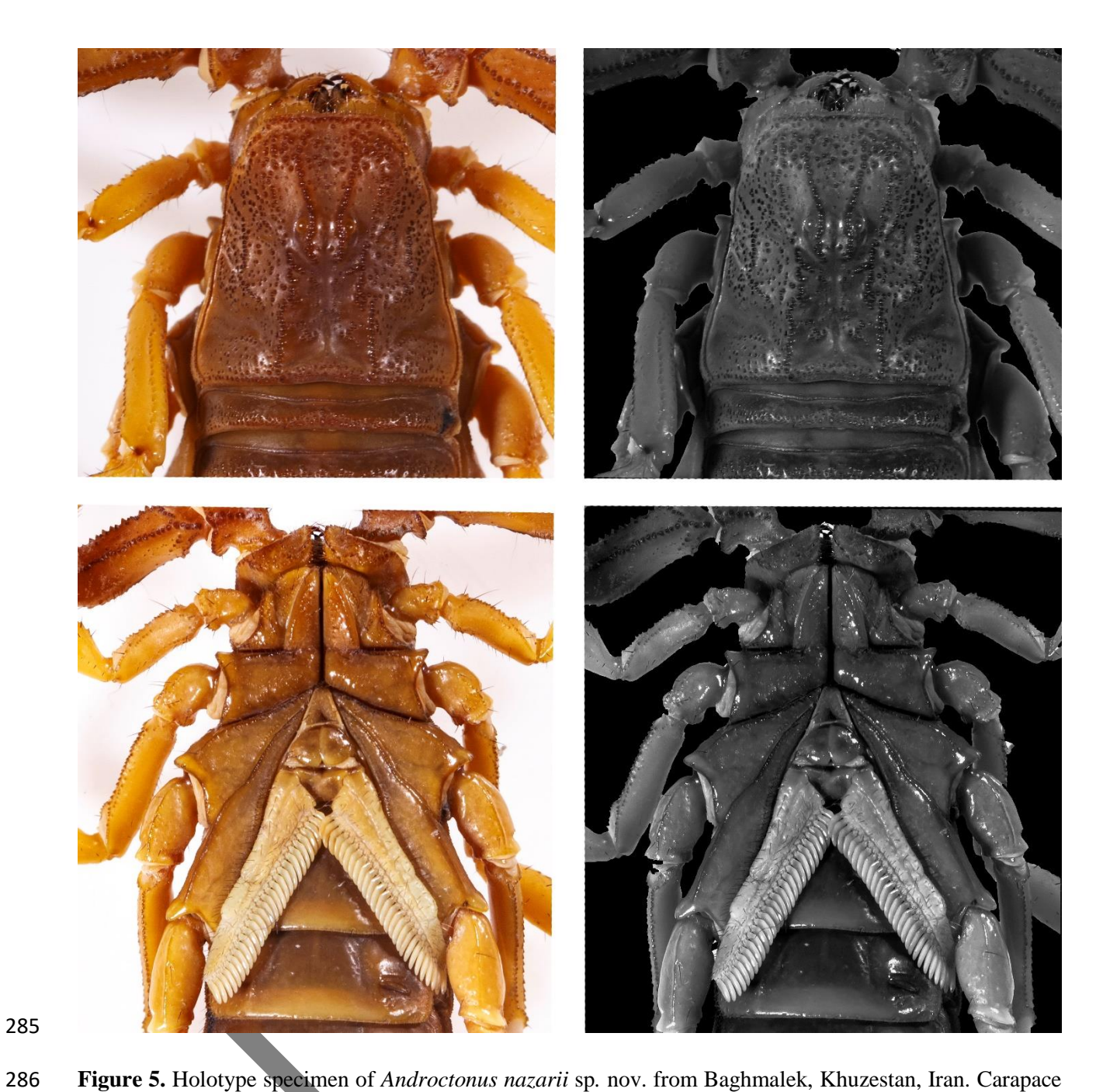


Figure 5. Holotype specimen of *Androctonus nazarii* sp. nov. from Baghmalek, Khuzestan, Iran. Carapace and sternopectinal area.



Figure 6. Holotype specimen of *Androctonus nazarii* sp. nov. from Baghmalek, Khuzestan, Iran. A. Dorsal view of pedipalp. B. Ventral view of pedipalp.

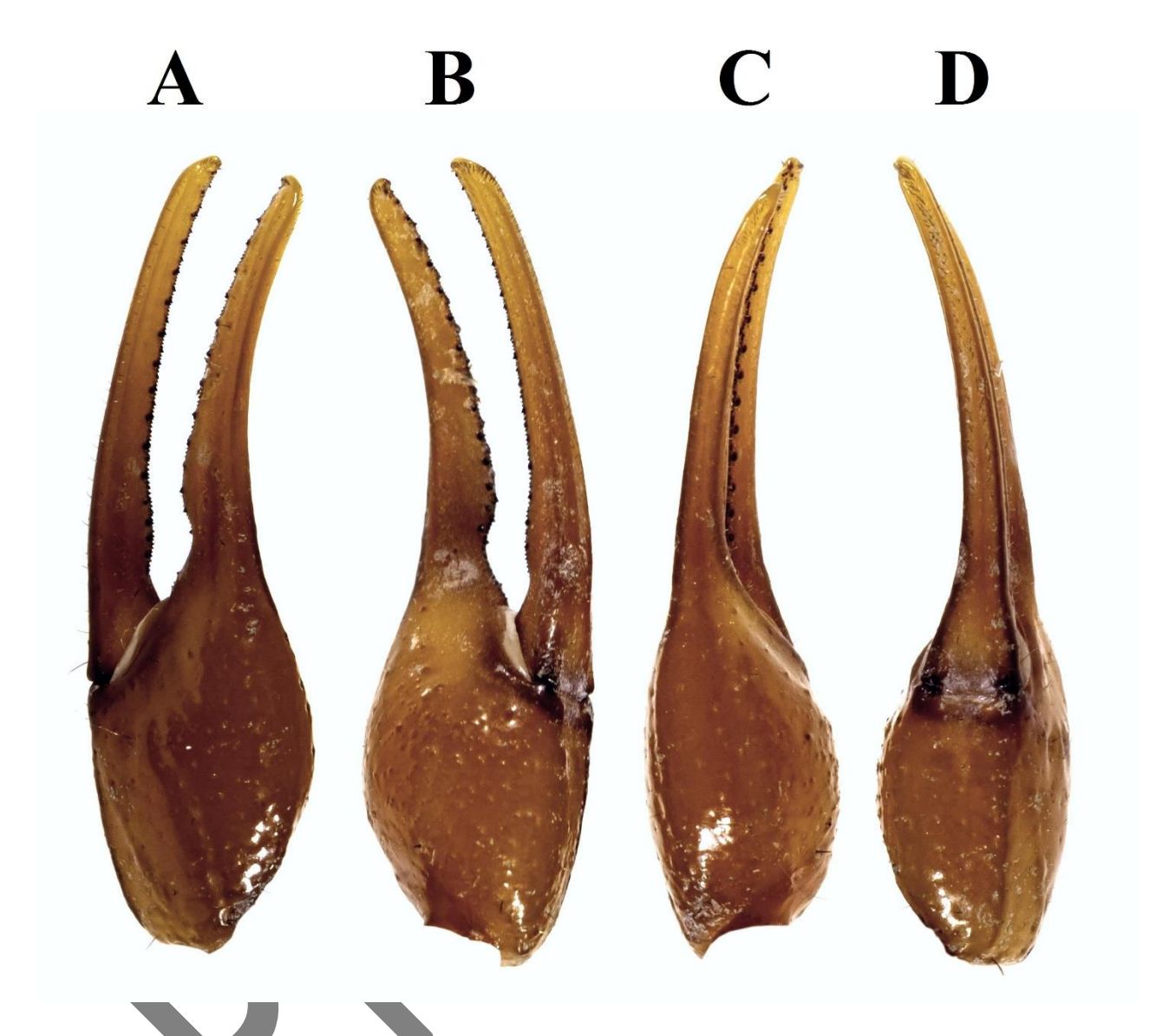


Figure 7. Holotype specimen of *Androctonus nazarii* sp. nov. from Baghmalek, Khuzestan, Iran. A. External view of chela. B. Internal view of chela. C. Dorsal view of chela. D. Ventral view of chela.

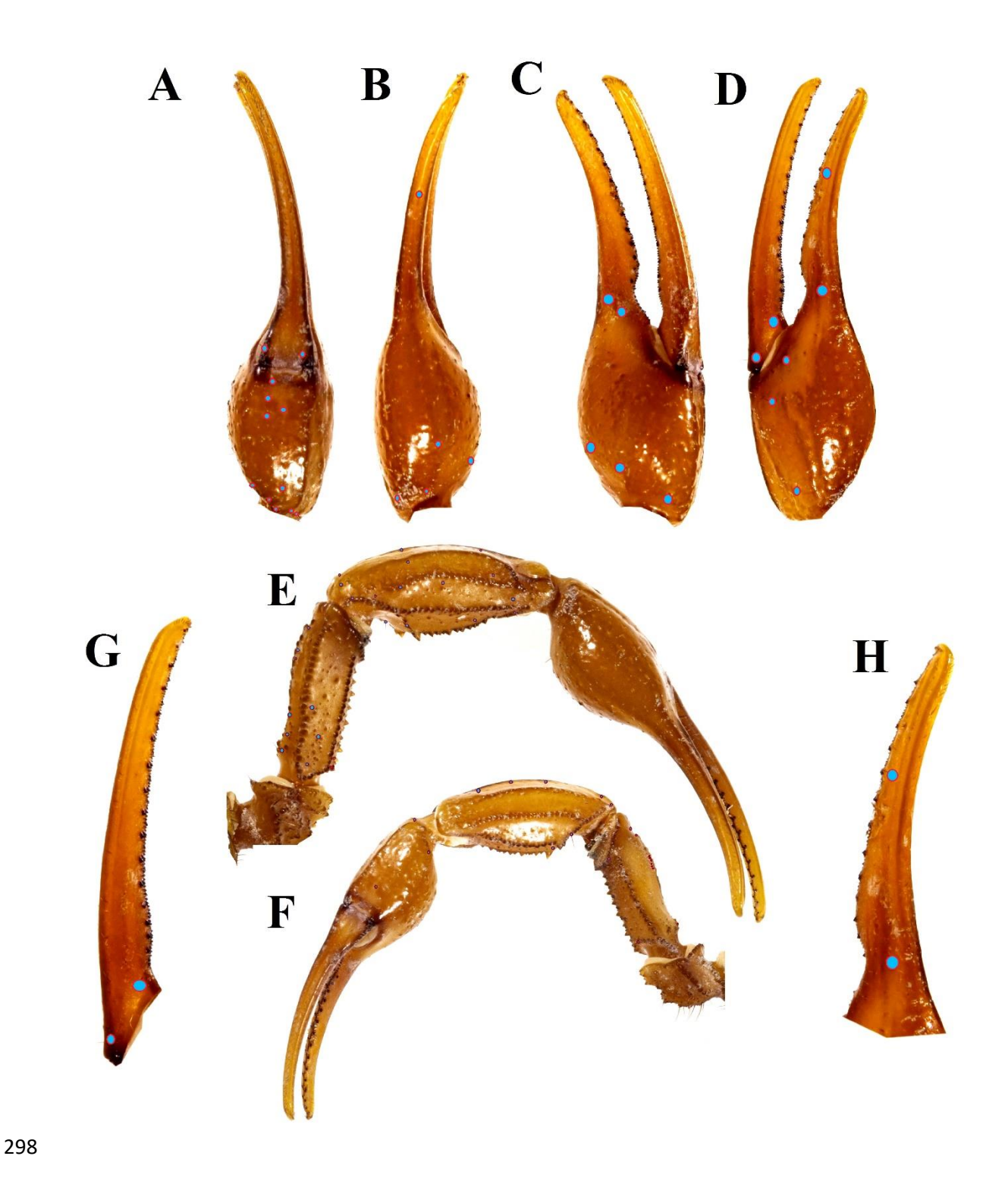


Figure 8. Holotype specimen of *Androctonus nazarii* sp. nov. from Baghmalek, Khuzestan, Iran. A. Ventral view of chela. B. Dorsal view of chela. C. Internal view of chela. D. External view of chela. E. Dorsal view of pedipalps. F. Ventral view of pedipalps. G. Movable finger dentition. H. Fixed finger dentition. Trichobothrial pattern is indicated by blue circles.

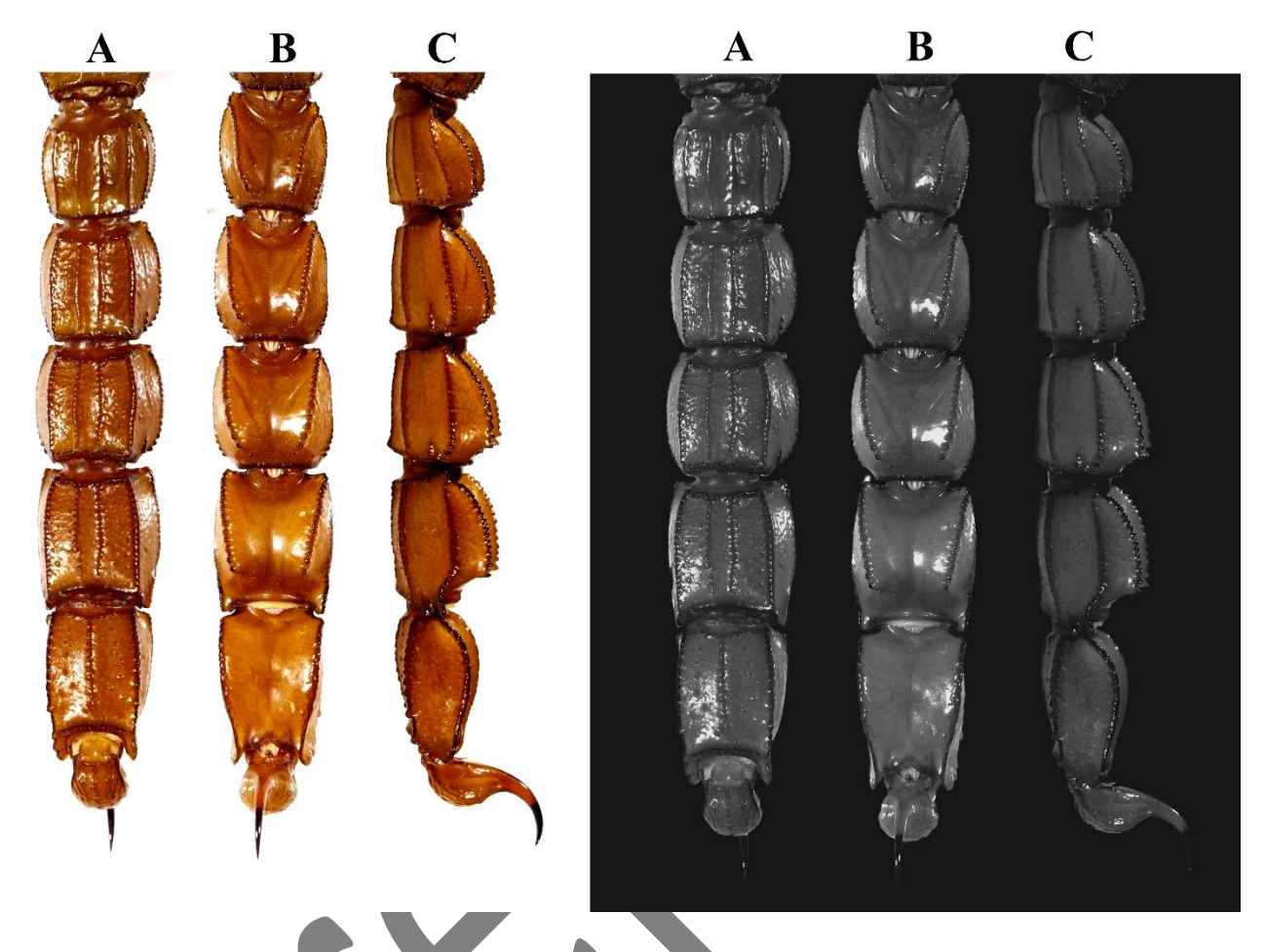


Figure 9. Holotype specimen of *Androctonus nazarii* sp. nov. from Baghmalek, Khuzestan, Iran. Metasoma and telson of adult male holotype. A. Ventral view; B. Dorsal view; C. Lateral view.



Figure 10. Holotype specimen of *Androctonus nazarii* sp. nov. from Baghmalek, Khuzestan, Iran. Right legs I–IV.

Affinities. A. nazarii sp. nov. can be distinguished from all other species of the genus by the following characters: The overall coloration is brownish-yellow (Figure 3), contrasting with the dark

brown of A. zagrosensis, A. barahoeii, and A. sumericus; the black of A. crassicauda; and the yellow 316 of A. sistanus. The carapace is predominantly light brown and lacks black patches, especially in the 317 ocular area, whereas it is dark brown to black with black patches in A. zagrosensis, A. barahoeii, A. 318 319 sumericus, A. crassicauda, A. orientalis, A. caspius, and A. azerianus; it is yellow but with ocular 320 black patches in A. sistanus. The carapace granulation in A. nazarii sp. nov. is dense and fine, lacking large anterior granules, unlike in A. zagrosensis, A. crassicauda, A. orientalis, A. azerianus, A. 321 barahoeii, A. caspius, and A. sumericus, which possess large, rounded anterior granules. All 322 segments of the legs are uniformly yellow in A. nazarii sp. nov. And A. sistanus, but brown in A. 323 sumericus, A. barahoeii, and A. zagrosensis. The metasoma and telson are yellowish-brown in A. 324 nazarii sp. nov., but reddish-brown in A. zagrosensis, A. sumericus, and A. barahoeii; in A. sistanus, 325 the overall color is yellow, but metasomal segments IV-V and the telson are black. The chela manus 326 is uniformly yellowish-brown in A. nazarii sp. nov., whereas it is uniformly reddish-brown with 327 black lines in A. zagrosensis (Figure 7), darker reddish-brown with spots and reticulations in A. 328 crassicauda, and uniformly brown to yellowish-brown in A. sumericus and A. barahoeii. The 329 internal surface of the chela manus is densely covered with fine granules in A. nazarii sp. nov., A. 330 331 crassicauda, A. barahoeii, and A. sumericus, but is smooth in A. zagrosensis. The pedipalp fingers are uniformly yellowish-brown in A. nazarii sp. nov., A. zagrosensis, A. barahoeii, and A. 332 333 sumericus, but black in A. crassicauda. Regarding the patella, in A. nazarii sp. nov. the dorsal, ventral, and external surfaces are smooth and the internal surface is finely granulated; in A. 334 335 zagrosensis all surfaces are smooth; and in A. sumericus and A. barahoeii it is granulate on the dorsal and internal surfaces but smooth externally. The intercarinal surface of tergite VII is smooth 336 337 in A. nazarii sp. nov., but granulated in A. barahoeii, A. crassicauda, A. orientalis, and A. sistanus. The sternites III-VII are uniformly colored with dull yellow posterior margins in A. nazarii sp. nov. 338 339 (Figures 4B, 4D), whereas sternites VI-VII are dark brown to black and lack posterior margins in A. 340 sumericus, A. barahoeii, and A. zagrosensis. The sixth sternite is smooth and lacks carinae in A. nazarii sp. nov. (Figures 4B, 4D), A. zagrosensis, A. barahoeii, and A. sumericus, but is carinate 341 and granulate in A. orientalis and A. crassicauda. The intercarinal surface of sternite VII is smooth 342 in A. nazarii sp. nov. (Figures 4B, 4D), A. zagrosensis, A. orientalis, and A. sumericus, but has fine 343 344 and abundant granules in A. crassicauda. For the metasoma, in A. nazarii sp. nov. segments I–V are smooth dorsally and laterally and granulate ventrally; in A. zagrosensis, segments I–IV are entirely 345 346 smooth and segment V is smooth dorsally and laterally but granulate ventrally; in A. sumericus, segments I–V are smooth dorsally but densely granulate laterally and ventrally; and in *A. barahoeii*, segments I–V are smooth dorsally and laterally, but segments II–V are granulate ventrally.

4. Discussion

347

348

349

350 The discovery of Androctonus nazarii sp. nov. from Baghmalek in Khuzestan Province is a 351 significant contribution to the ongoing revision of the A. crassicauda species complex in Iran and the broader Middle East. This finding underscores the cryptic diversity within the genus 352 Androctonus, a pattern that has become increasingly apparent through recent integrative taxonomic 353 studies [15, 17, 20, 22]. For years, populations in southwestern Iran were inconsistently reported 354 355 under the name A. crassicauda [1, 14], obscuring the true species richness of the region. The present study clarifies the taxonomic identity of the Baghmalek population, confirming it as a distinct 356 species that is morphologically separable from its congeners, particularly the recently described 357 sympatric and parapatric species A. zagrosensis, A. barahoeii, and A. sumericus. 358 The distinct morphological identity of A. nazarii sp. nov. is established by a suite of diagnostic 359 360 characters, most notably its unique coloration and granulation patterns. The overall brownish-yellow coloration provides an immediate and stark contrast to the dark brown of A. zagrosensis, A. 361 barahoeii, and A. sumericus, the black of A. crassicauda, and the uniform yellow of A. sistanus. 362 Critically, the carapace of A. nazarii sp. nov. lacks the large, rounded anterior granules that are 363 364 characteristic of nearly all its regional congeners, including A. zagrosensis, A. barahoeii, A. sumericus, and A. crassicauda. Instead, it exhibits dense, fine granulation. This character alone is a 365 366 powerful diagnostic tool. Furthermore, the absence of black patches in the ocular area distinguishes it from species like A. sistanus, which, despite having a yellow carapace, retains these distinctive 367 368 patches. The unique identity of A. nazarii sp. nov. is further solidified by distinct morphological 369 370 characteristics of its pedipalps and metasoma. Its chela manus is uniformly yellowish-brown, distinguishing it from the marked manus of relatives like A. zagrosensis and A. crassicauda. 371 Furthermore, a unique combination of granulation patterns—specifically, a smooth intercarinal 372 surface on both tergite VII and sternite VII, coupled with metasomal segments that are smooth 373 374 dorsally and laterally but granulate ventrally, creates a morphological profile not found in any compared species. The description of A. nazarii sp. nov. from Baghmalek adds another piece to the 375 complex biogeographic puzzle of the Zagros Mountains and the Khuzestan Plain. The fact that 376 multiple morphologically distinct Androctonus species (A. nazarii sp. nov., A. zagrosensis, A. 377

barahoeii) have been identified in relatively close proximity within the Zagros range suggests that this region has acted as a cradle for allopatric speciation, potentially driven by microhabitat specialization or historical vicariance events. The sympatric report of *A. sumericus* and *A. barahoeii* in other parts of Khuzestan [15, 20] further highlights the province as a significant biodiversity hotspot for scorpions, requiring careful species-level identification for accurate distribution records. In conclusion, the identification of *Androctonus nazarii* sp. nov. reaffirms that the taxonomic resolution of the *A. crassicauda* complex is far from complete. It demonstrates that even within a well-studied country like Iran, and in a genus of significant medical concern, new species await discovery in regions with complex topography. Future research should employ molecular phylogenetics to corroborate the morphological species boundaries proposed here and to elucidate the evolutionary relationships within this rapidly diversifying species group. Such integrative approaches will be essential for a comprehensive understanding of *Androctonus* diversity, biogeography, and its implications for human health.

390 391

392

378

379

380

381

382

383

384

385

386

387

388

389

Acknowledgments

- The authors sincerely thank Sina Taghavi Moghadam for his valuable collaboration in this research.
- We also wish to posthumously honor and dedicate this work to the memory of the late Dr. Ahmad
- 395 Taghavi Moghadam. Furthermore, we are grateful to the Razi Vaccine and Serum Research
- Institute, Agricultural Research, Education and Extension Organization (AREEO), in Karaj, Iran,
- for their support with laboratory equipment and facilities.

Funding

Research conducted at Razi Vaccine and Serum Research Institute without external funding.

399 400

401

398

Ethics declarations

- 402 All sample collection methods and experimental procedures described herein were rigorously
- 403 reviewed and approved by the Institutional Animal Care Committee of Razi Vaccine and Serum
- 404 Research Institute (Permit number IR.RVSRI.REC.1401.017) and AREEO protocols, which comply
- with Iran guidelines for work with animals.

406 Authors' Contribution

- Study concept and design: F S and SM K. Gathering and coding the data: F S, SM K, AR F, B Z,
- 408 MH JM. Analysis and interpretation of data: F S. Photography: B Z. Drafting of the manuscript: F
- 409 S and SM K. Revision of the manuscript: F S, MH JM, SM K.

410 Conflicts of Interest

The authors declared that they have no conflict of interest.

412 **Data Availability**

- The data that support the findings of this study are available on request from the corresponding
- 414 author.

415

416 References

- 1. Salabi F, Jafari H, Mahdavinia M, Azadnasab R, Shariati S, Baghal ML, et al. First
- 418 transcriptome analysis of the venom glands of the scorpion *Hottentotta zagrosensis* (Scorpions:
- Buthidae) with focus on venom lipolysis activating peptides. Front Pharmacol. 2024;15:1464648.
- 420 2. Salabi F, Vazirianzadeh B, Baradaran M. Identification, classification, and characterization of
- alpha and beta subunits of LVP1 protein from the venom gland of four Iranian scorpion species. Sci
- 422 Rep. 2023;13(1):22277.
- 3. Salabí F, Jafari H. Whole transcriptome sequencing reveals the activity of the PLA2 family
- 424 members in Androctonus crassicauda (Scorpionida: Buthidae) venom gland. FASEB J.
- 425 2024;38(10):e23658.
- 426 4. Salabi F, Jafari H. Dataset of PLA2 family identified from transcriptomic high-throughput
- 427 sequencing of Androctonus crassicauda (Scorpionida: Buthidae) venom gland. Data Brief.
- 428 2024;55:110629.
- 429 5. Olson DM, Dinerstein E, Wikramanayake ED, Burgess ND, Powell GVN, Underwood EC, et
- al. Terrestrial ecoregions of the world: a new map of life on Earth. Bioscience. 2001;51(11):933-
- 431 938.

- 432 6. Safaei-Mahroo B, Ghaffari H, Fahimi H, Broomand S, Yazdanian M, NajafiMajd E, et al. The
- Herpetofauna of Iran: Checklist of Taxonomy, Distribution and Conservation Status. Asian Herpetol
- 434 Res. 2015;6(4):257–290.
- 435 7. Kazemi SM, Hosseinzadeh MS, Weinstein SA. Identifying the geographic distribution pattern
- of venomous snakes and regions of high snakebite risk in Iran. Toxicon. 2023;231:107197.
- 8. Kazemi SM, Sabatier JM. Venoms of Iranian Scorpions (Arachnida, Scorpiones) and Their
- 438 Potential for Drug Discovery. Molecules. 2019;24(14):2670.
- 9. Baradaran M, Salabi F, Mahdavinia M, Mohammadi E, Vazirianzadeh B, Avella I, et al.
- 440 ScorpDb: A Novel Open-Access Database for Integrative Scorpion Toxinology. Toxins.
- 441 2024;16(11):497.
- 442 10. Kazemi SM, Lari Baghal M, Salabi F. Androctonus zagrosensis sp. nov., a new medically
- important scorpion species from Khuzestan Province, Iran (Scorpiones: Buthidae). J Nat Hist.
- 444 Forthcoming 2025.
- 11. Prendini L. Phylogeny of *Parabuthus* (Scorpiones, Buthidae). Zool Scr. 2001;30(1):13-35.
- 12. Lourenço WR, Qi JX. A new species of Androctonus Ehrenberg, 1828 from Afghanistan
- 447 (Scorpiones, Buthidae). Zool Middle East. 2006;38(1):93-97.
- 13. Olivier GA. Voyage dans l'Empire Othoman, l'Egypte et la Perse. Paris: Henri Agasse; 1807.
- 14. Gharakhloo MM, Heydaraba SA, Yağmur EA. The scorpion fauna of West Azerbaijan Province
- in Iran (Arachnida: Scorpiones). Biharean Biol. 2018;12(2):84-87.
- 451 15. Yağmur EA, Kovařík F, Fet V, Lowe G, Moradi M, Kalami F. A review of Androctonus of
- 452 Iran, with redescription of A. crassicauda (Olivier, 1807) and A. orientalis (Birula, 1900) stat. n.,
- and descriptions of four new species (Scorpiones: Buthidae). Euscorpius. 2025;(422):1-69.
- 16. Yağmur EA, Kachel HS, Al-Khazali AM, Al-Jubouri MAK, Ali FR. Androctonus Ishtar sp. n.
- from Dohuk and Nineveh provinces, Iraq (Scorpiones: Buthidae). J Nat Hist. 2025;59(25-28):1757-
- 456 1773.
- 457 17. Lowe G. The genus Androctonus Ehrenberg, 1828 (Scorpiones: Buthidae) in Oman.
- 458 Euscorpius. 2025;(424):1-59.
- 459 18. Al-Khazali AM, Yağmur EA. Androctonus sumericus sp. nov., a new scorpion from Dhi Qar
- 460 Province, Iraq (Scorpiones: Buthidae). Zool Middle East. 2023;69(4):410-419.
- 461 19. Alqahtani AR, Yağmur EA, Badry A. Androctonus tihamicus sp. nov. from the Mecca Province,
- Saudi Arabia (Scorpiones, Buthidae). ZooKeys. 2023;1152:9-34.

- 20. Barahoei H, Mirshamsi O, Amiri M, Moeinadini A, Rakhshani E. Integrative taxonomy reveals
- the existence of a new species of fat-tailed scorpions, *Androctonus* (Buthidae), in Iran. Turk J Zool.
- 465 2025;49(2):48-74.
- 466 21. Birula A. Beiträge zur Kenntniss der Scorpionenfouna Ost-Persiens. Bull Acad Imp Sci St-
- 467 Pétersbourg. 1900;12(4):355-375.
- 468 22. Salabi F. A computational study of venom as drug library: discovery of multifunctional astacin-
- like metalloproteases from *Androctonus zagrosensis* venom gland transcriptome. Comput Biol Med.
- 470 2025;198:111247.
- 471 23. Kazemi SM, Gholam Kelisani Z, Avella I, Lüddecke T. The need for a refined scorpion
- antivenom for Iran. Toxicon 2024; 248: 108033.
- 473 24. Barahoei H, Navidpour S, Aliabadian M, Siahsarvie R, Mirshamsi O, Scorpions of Iran
- 474 (Arachnida: Scorpiones): Annotated checklist, DELTA database and identification key. J Insect
- 475 Biodivers Syst. 2020;6(4):375–474.
- 476 25. Sissom WD, Polis GA, Watt DD. Field and laboratory methods. In: Polis GA, editor. The
- Biology of Scorpions. Stanford (CA): Stanford University Press; 1990. p. 215-221.
- 478 26. Yağmur EA. Androctonus turkiyensis sp. n. from the Şanlıurfa Province, Turkey
- 479 (Scorpiones:Buthidae). Euscorpius. 2021;(341):1–18.